CYTOKININ RESPONSE FACTOR2 (CRF2) and CRF3 Regulate Lateral Root Development in Response to Cold Stress in Arabidopsis

Jin Jeon,[a,1] Chuloh Cho,[a,1] Mi Rha Lee,[a] Nguyen Van Binh,[a] and Jungmook Kim[a,b,2]

[a] Department of Bioenergy Science and Technology, Chonnam National University, Buk-Gu, Gwangju 500-757, Korea
[b] Kumho Life Science Laboratory, Chonnam National University, Buk-Gu, Gwangju 500-757, Korea

ORCID IDs: 0000-0001-7997-1544 (C.C.); 0000-0003-1735-5564 (J.K.)

Lateral roots (LRs) are a major determinant of the root system architecture in plants, and developmental plasticity of LR formation is critical for the survival of plants in changing environmental conditions. In *Arabidopsis thaliana*, genetic pathways have been identified that regulate LR branching in response to numerous environmental cues, including some nutrients, salt, and gravity. However, it is not known how genetic components are involved in the LR adaptation response to cold. Here, we demonstrate that *CYTOKININ RESPONSE FACTOR2* (*CRF2*) and *CRF3*, encoding APETALA2 transcription factors, play an important role in regulating Arabidopsis LR initiation under cold stress. Analysis of LR developmental kinetics demonstrated that both *CRF2* and *CRF3* regulate LR initiation. *crf2* and *crf3* single mutants exhibited decreased LR initiation under cold stress compared with the wild type, and the *crf2 crf3* double mutants showed additively decreased LR densities compared with the single mutants. Conversely, *CRF2* or *CRF3* overexpression caused increased LR densities. *CRF2* was induced by cold via a subset of the cytokinin two-component signaling (TCS) pathway, whereas *CRF3* was upregulated by cold via TCS-independent pathways. Our results suggest that *CRF2* and *CRF3* respond to cold via TCS-dependent and TCS-independent pathways and control LR initiation and development, contributing to LR adaptation to cold stress.

INTRODUCTION

The plant root system is important for the anchorage of plants in soil and the uptake of water and nutrients (Hochholdinger and Zimmermann, 2008). The root system of dicotyledonous plants is made up of a primary root and lateral roots (LRs). LRs are a major determinant of the root system architecture in plants (Péret et al., 2009a). In *Arabidopsis thaliana*, LRs originate from founder cells formed from xylem pole pericycle cells primed in the basal meristem and undergo anticlinal and asymmetric division to create single layered primordia. These cells undergo further anticlinal and periclinal divisions to generate a dome-shaped LR primordium (LRP) that emerges from the primary root via cell separation (Parizot et al., 2008; Péret et al., 2009a, 2009b; Lavenus et al., 2013). The process of Arabidopsis LR development is critically regulated by auxin, mainly via two AUXIN/INDOLE-3-ACETIC ACID (Aux/IAA)-AUXIN RESPONSE FACTOR (ARF) modules including SOLITARY-ROOT/IAA14-ARF7-ARF19 and BODENLOS/IAA12-ARF5 (Fukaki et al., 2002; Vanneste et al., 2005; De Smet et al., 2010).

Abiotic stresses including cold stress and the availability of nutrients are known to modulate the root system architecture of plants. Plants exposed to low temperature produce smaller root systems and roots of thinner diameter (Pahlavanian and Silk, 1988;

Nagel et al., 2009). Low temperature reduces the biomass in the basal parts of root systems and in lateral roots and induces smaller branching angles between the primary and lateral roots (Nagel et al., 2009). Cold stress inhibits root basipetal auxin transport by reducing the trafficking of the auxin efflux carrier PIN2 and inhibiting the lateral relocalization of PIN3 in Arabidopsis (Shibasaki et al., 2009). Cold reduces both root meristem size and cell number, repressing the division potential of meristematic cells by reducing auxin accumulation (Zhu et al., 2015). Thus, cold stress inhibits root growth partly by modulating auxin synthesis, transport, and response.

Cytokinin and a subset of a two-component signaling (TCS) system are involved in cold stress signaling and response (Jeon et al., 2010; Shi et al., 2012; Jeon and Kim, 2013). In Arabidopsis, cytokinins use a multistep TCS system that comprises the three sensor histidine kinases ARABIDOPSIS HISTIDINE KINASEs (AHKs) AHK2, AHK3, and AHK4 (Inoue et al., 2001; Suzuki et al., 2001; Ueguchi et al., 2001; Yamada et al., 2001; Kakimoto, 2003), five HISTIDINE PHOSPHOTRANSFER PROTEINs (AHPs) mediating the transfer of phosphoryl groups from AHKs to ARABIDOPSIS RESPONSE REGULATORs (ARRs) (To and Kieber, 2008), and three types of ARRs classified into type-A, type-B, and type-C (Pils and Heyl, 2009). The type-B ARRs (ARR1, 2, 10-14, and 18-21) are transcription factors that function as positive regulators of cytokinin signaling (Hwang et al., 2012). The type-A ARRs (ARR3-9 and 15-17) are rapidly and transiently induced by cytokinin treatment and function as negative regulators of cytokinin signaling (Kiba et al., 2003; To et al., 2004; Lee et al., 2007; Hwang et al., 2012). The type-C ARRs (ARR22 and ARR24) have a domain structure similar to that of the type-A ARRs, but their expression is not induced by cytokinins (Kiba et al., 2004; Horák et al., 2008; Pils and Heyl, 2009). Although

the role of type-C *ARR*s in cytokinin signaling is unclear, it has been proposed that *ARR22* plays a positive role in the stress tolerance response (Kang et al., 2012). A subset of the Arabidopsis cytokinin TCS system is utilized for cold stress signaling and response (Jeon et al., 2010; Jeon and Kim, 2013; Zhu et al., 2015). ARR1 mediates the cold signal via AHP2, AHP3, or AHP5 from AHK2 and AHK3 to express a subset of type-A *ARR*s, regulating cold stress response and tolerance along with cytokinin (Jeon et al., 2010; Jeon and Kim, 2013). ARR1 and ARR12 are also involved in the inhibition of Arabidopsis root growth by low temperature (Zhu et al., 2015).

Analysis of the cold transcriptome affected by *ahk2 ahk3* mutations revealed a cold-responsive gene network regulated downstream of AHK2 and AHK3. *CYTOKININ RESPONSE FACTOR2* (*CRF2*), encoding a member of the *APETELA2* (*AP2*)/*ETHYLENE RESPONSE FACTOR* (*ERF*) transcription factors, was found to be downregulated by *ahk2 ahk3* mutations in response to cold, indicating that cold-responsive expression of *CRF2* is regulated downstream of AHK2 and AHK3 (Jeon and Kim, 2013). Some *CRF* members, such as *CRF1*, *CRF2*, and *CRF5*, play a role in the development of the cotyledon, leaf, and embryo (Rashotte et al., 2006). *CRF2*, *CRF5*, and *CRF6*, but not *CRF1*, *CRF3*, or *CRF4*, were upregulated by cytokinins (Rashotte et al., 2006). Microarray analysis of *arr1,12*, *crf1,2,5*, and *crf2,3,6* with or without cytokinin benzyladenine revealed that some CRF members act in parallel with type-B ARRs to mediate cytokinin-regulated gene expression and also coregulate the target genes with type-B ARRs (Rashotte et al., 2006). The AP2/ERF family transcription factors have been implicated in the response to plant hormones and as mediators of stress responses and developmental processes (Mizoi et al., 2012; Licausi et al., 2013).

Here, we show that cold induces the expression of *CRF2* and *CRF3*, which are involved in LR initiation and LR formation, via TCS-dependent and TCS-independent signal transduction pathways, respectively, and that *CRF2* and *CRF3* promote LR initiation under cold stress. Cold-responsive *CRF2* expression is affected by mutations in *AHK2* and *AHK3* as well as in *AHP2*, *AHP3*, and *AHP5*, indicating that the TCS pathway is involved in regulating *CRF2* expression in response to cold. We further showed that ARR1 directly regulates *CRF2* expression by binding to the *CRF2* promoter. By contrast, the cold response of *CRF3* expression is not altered by mutations in the TCS signaling components. Mutations in *CRF2* and *CRF3* cause a delay in LR initiation and a reduction in LR formation, whereas overexpression of *CRF2* or *CRF3* in Arabidopsis enhances LR initiation and LR formation. The *crf2* and *crf3* single and double mutants display a hypersensitive response in LR initiation events to cold stress compared with that of the wild type, whereas overexpression of *CRF2* or *CRF3* enhances LR initiation under cold stress. Based on these results, we propose that *CRF2* and *CRF3* integrate the environmental cold signal into LR development and mediate the adaptation to cold stress to influence changes in root system architecture and limit the negative effects of cold on root growth.

RESULTS

CRF2 and *CRF3* Respond to Cold

The Arabidopsis *CRF* gene family comprises 12 members (Rashotte and Goertzen, 2010; Zwack et al., 2012). We first examined the expression profiling of *CRF*s using the Genevestigator Web tool, which provides a summary of gene expression responses to a variety of stimuli, in order to identify the *CRF* genes that are responsive to cold. Figure 1A shows the responses of *CRF*s to phytohormones and abiotic stresses including cold. *CRF2*, *CRF3*, *CRF6*, and *CRF10* exhibited cold response, and in particular, *CRF2* and *CRF3*, a close homolog to *CRF2*, showed strong induction by cold (Figure 1A). We determined cold-responsive expression of *CRF2* and *CRF3* by conducting RT-qPCR for the plants treated with cold for varying times. *CRF2* and *CRF3* showed a transient change in gene expression with maximum response occurring with 4 h of cold treatment (Figure 1B). *CBF1* was used as a cold marker gene to confirm the effect of the cold treatment with regard to the induction of gene expression. Both *CRF2* and *CRF3* exhibited significant cold-responsive gene expression in both the shoot and the root, although *CRF2* showed higher levels of cold response in the shoot compared with that in the root (Figure 1C).

CRF2 and *CRF3* Are Expressed via Different Cold Signaling Pathways

To determine whether TCS components are involved in cold-inducible expression of *CRF2* and *CRF3*, we analyzed the expression of *CRF2* and *CRF3* in *ahk*, *ahp*, and type-B *arr* mutants using RT-qPCR. Plants were treated with cold for 4 h, corresponding to peak expression in wild-type plants (Figure 1B). The *ahk2 ahk3* double mutants exhibited significantly reduced *CRF2* expression in response to cold compared with that in the wild type (Figure 2A). The *ahp2 ahp3 ahp5* triple mutants also showed significantly reduced cold-responsive expression of *CRF2* and the *ahp1 ahp2 ahp3 ahp4 ahp5* quintuple mutants displayed more reduced *CRF2* expression than that in the triple mutants (Figure 2B). All of the mutants are in the Col-0 accession except for *ahp1-1*, which is in the Wassilewskija-2 background. Although there are multiple genetic differences between Col-0 and Ws that could influence the interaction with the quintuple mutant and *CRF2* expression, this is unlikely given the comparison to each respective wild type (Figure 2B). *CRF2* expression was also reduced in the type-B *arr* mutants such as *arr1*, *arr10*, and *arr12* single mutants and *arr1 arr10*, *arr1 arr12*, and *arr10 arr12* double mutants and even more reduced in *arr1 arr10 arr12* triple mutants, indicating that *ARR1*, *ARR10*, and *ARR12* in part redundantly regulate *CRF2* expression in response to cold (Figure 2C). By contrast, *CRF3* expression in response to cold was not altered in any of these TCS mutants compared with that of the wild type. These results indicated that TCS is involved in mediating the cold signal for expressing *CRF2*, whereas cold-responsive expression of *CRF3* occurs independently of the TCS system.

CRF protein subcellular localization assays have previously shown that cytokinin rapidly induces the relocalization of CRF2, CRF3, and CRF6 into the nucleus and that both AHPs and cytokinin receptors are required for the cytokinin-regulated movement of CRF2 into the nucleus (Rashotte et al., 2006). We analyzed the subcellular distribution of EGFP:CRF2 and EGFP:CRF3 in the wild-type Arabidopsis mesophyll protoplasts without or with cold treatment by confocal scanning laser microscopy, showing that both CRF2 and CRF3 were localized in both the cytosol and the
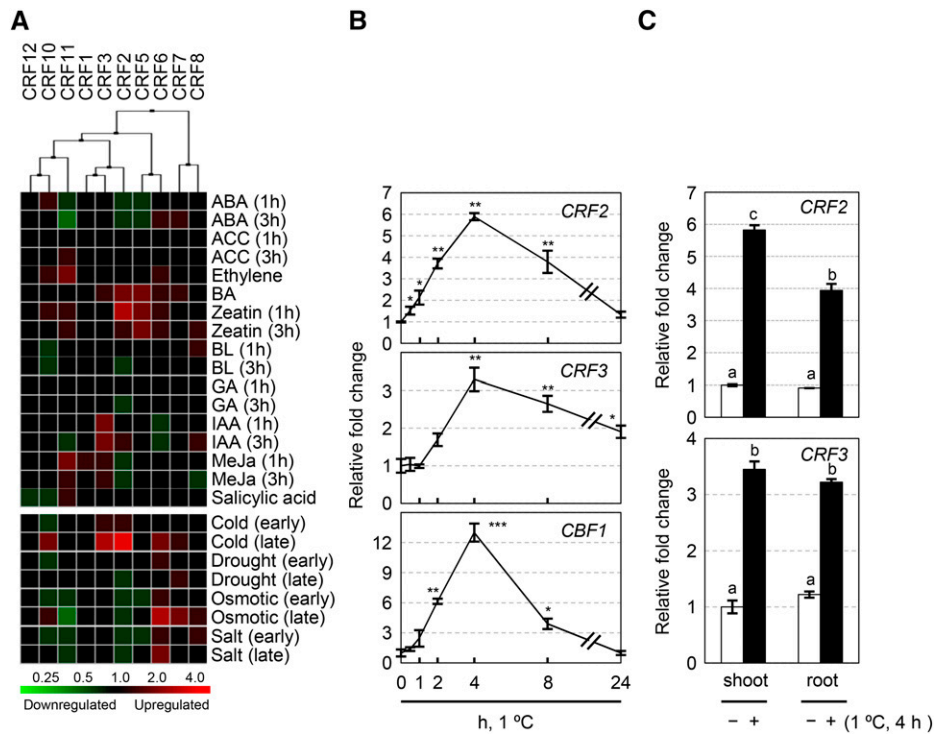
Figure 1. Expression Analysis of *CRF* Genes.

(A) Hierarchical cluster analysis of the *CRF* genes in response to phytohormones and abiotic stresses. The response of the *CRF* genes to a given stimulus was obtained from Genevestigator. "Early" and "late" indicate the samples which were treated for 30 min, 1 h, or 3 h and combined, and the samples which were treated for 6, 12, or 24 h and combined, respectively.

(B) and **(C)** RT-qPCR analysis of *CRF2* and *CRF3* expression in response to cold in 10-d-old whole plants sampled three times over a 24-h cold exposure period **(B)** and in shoot and root tissue isolated from 8-d-old plants after a 4-h cold exposure **(C)**. Relative fold changes were plotted as the ratio of the given treatment relative to the transcript level at 0 h, after normalization to *ACTIN7*. Mean $\pm$ SE values were determined from n = three biological replicates (each biological replicate was estimated as the average of two technical RT-qPCR replicates). Asterisks in **(B)** indicate significant differences compared with the wild type at 0 h using Student's t test (*$P < 0.05$; **$P < 0.01$; ***$P < 0.001$). As a measure of absolute expression levels, the copy numbers at 0 h were 308 for *CBF1*, 1082 for *CRF2*, 931 for *CRF3*, and 12,833 for *ACTIN7*. Bars with different letters in **(C)** indicate significant differences at $P < 0.05$ by two-way ANOVA and the Tukey's honestly significant difference test (Supplemental Figure 9).

nucleus and that cold treatment did not affect the subcellular distribution of these two CRFs (Supplemental Figure 1).

ARR1 Regulates *CRF2* Expression by Directly Binding to the *CRF2* Promoter

As *ARR1* in combination with *ARR10* and *ARR12* are redundantly involved in cold-responsive expression of *CRF2* (Figure 2C) and *ARR1* has been shown to play a key role in cold-responsive expression of type-A *ARR*s (Jeon and Kim, 2013), we investigated whether ARR1 directly regulates *CRF2* expression. We generated transgenic Arabidopsis expressing ARR1 tagged with 10 copies of MYC epitopes in frame with ARR1 N terminus in *arr1-3* mutants (*Pro35S:10xMYC:ARR1/arr1-3*) to test whether *ARR1* expression rescues the reduced cold-responsive expression of *CRF2* in *arr1* mutants compared with that in the wild type (Supplemental Figure 2). The *arr1* mutants and *Pro35S:10xMYC:ARR1/arr1-3* plants were treated with cold for 0, 2, 4, or 24 h, and *CRF2* expression was determined by RT-qPCR compared with that in the wild type (Figure 3A). *arr1* mutants showed reduced expression of *CRF2*

after 2 and 4 h of cold treatment, whereas *Pro35S:10xMYC:ARR1/arr1-3* plants exhibited wild-type response of *CRF2* expression to cold. However, *CBF1* was expressed at the same levels in response to cold in wild-type, *arr1*, and *Pro35S:10xMYC:ARR1/arr1-3* plants. These results demonstrated that *ARR1* positively regulates *CRF2* expression in response to cold.

To prove whether ARR1 upregulates *CRF2* expression via the *CRF2* promoter, we used Arabidopsis protoplast transient gene expression assays with a reporter plasmid harboring the *CRF2* promoter fused to *LUC* (*ProCRF2:LUC*) and an effector plasmid harboring *ARR1* under the control of the CaMV 35S promoter (*Pro35S:Ω:4xHA:ARR1*). *ARR1* expression resulted in a 70-fold enhancement of *LUC* expression from *ProCRF2:LUC*, whereas the coexpression of *ProCRF2:LUC* with a negative control, *Pro35S:Ω:3xHA:EGFP*, did not enhance *LUC* expression (Figure 3B). This result demonstrated that ARR1 upregulates *CRF2* expression through the *CRF2* promoter. To examine whether ARR1 directly upregulates *CRF2* expression, we analyzed *CRF2* expression in transgenic Arabidopsis overexpressing ARR1ΔDDK fused with the glucocorticoid receptor hormone binding
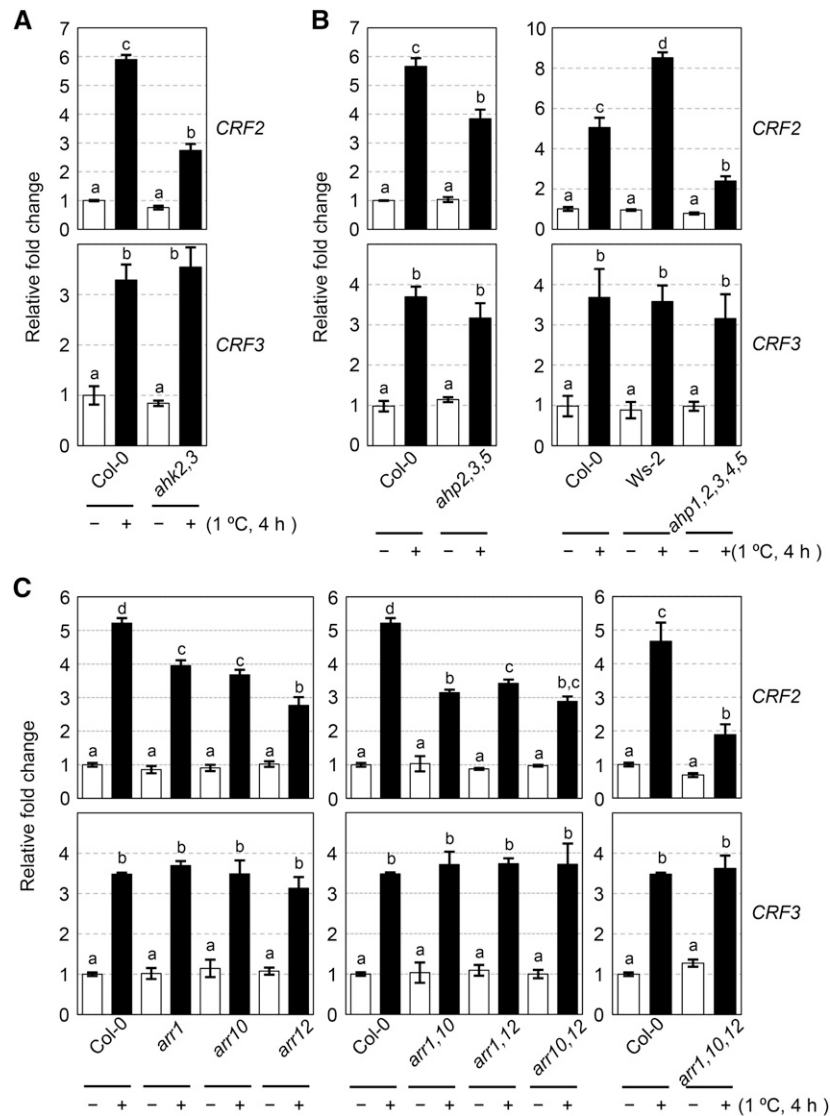
Figure 2. Expression of *CRF2* and *CRF3* in Two-Component Signaling Mutants in Response to Cold.

Expression of *CRF2* and *CRF3* in wild-type (Col-0 or Ws as indicated) and *ahk2-2 ahk3-3* double mutants **(A)**, *ahp* triple and pentuple mutants **(B)**, and *arr* single, double, and triple mutants **(C)** treated for 0 or 4 h at 1°C. Ten-day-old plants were treated for 4 h at 1°C and subjected to RT-qPCR analysis. Relative fold changes were plotted after normalization to *ACTIN7*. Bars with different letters indicate significance at P < 0.01 by two-way ANOVA and the Tukey's honestly significant difference test (Supplemental Figure 9). All panels show mean ± sᴇ values determined from *n* = three biological replicates (each biological replicate was estimated as the average of two technical RT-qPCR replicates).

domain (GR), but without the ARR1 receiver domain (*Pro₃₅ₛ:ARR1ΔDDK:GR*) in a dexamethasone (DEX)-inducible manner (Jeon and Kim, 2013). DEX treatment of *Pro₃₅ₛ:ARR1ΔDDK:GR* plants induced the expression of *CRF2* by 3-fold compared with that in mock-treated transgenic plants (Figure 3C). While the treatment of cycloheximide, a protein synthesis inhibitor, of *Pro₃₅ₛ:ARR1ΔDDK:GR* plants resulted in increased *CRF2* expression, cycloheximide did not prevent the DEX-induced expression of *CRF2*. These results indicated that *CRF2* is a primary response gene directly regulated by ARR1 without new protein synthesis.

We identified eleven putative ARR1 binding sites harboring the conserved 5′-AGATT-3′ sequence element in the 2-kb *CRF2* promoter region relative to the AUG codon (Figure 3D). To determine whether ARR1 can directly bind to these ARR1 binding sites in the *CRF2* promoter, we first performed an electrophoretic mobility shift assay (EMSA) using truncated ARR1 recombinant protein encompassing 300 amino acids from the N terminus fused with GST. We selected a particular region harboring the ARR1 binding site (indicated by the arrowhead A in Figure 3D) and prepared 29-mer of oligonucleotide DNA probe (probe A) from the *CRF2* promoter sequences for EMSA. GST-ARR1 was shown to
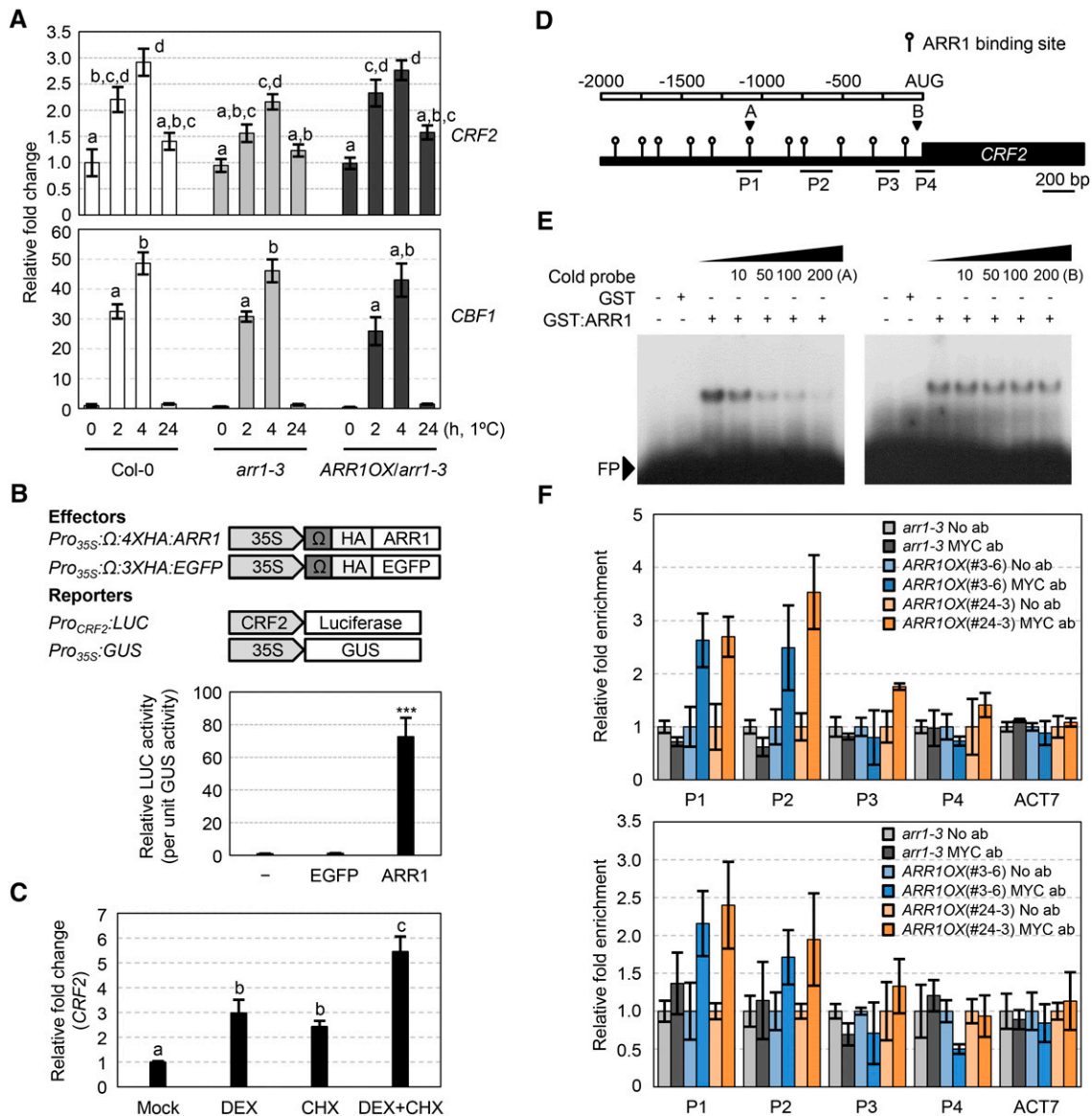
Figure 3. ARR1 Regulates *CRF2* Expression by Directly Binding to the *CRF2* Promoter.

(A) Expression analysis of *CRF2* in *arr1-3* mutants and *Pro35S:10xMYC:ARR1*(*ARR1OX*)/*arr1-3* plants in response to cold. Mean ± se values determined from *n* = three biological replicates (each biological replicate was estimated as the average of two technical RT-qPCR replicates). Relative fold change represents the ratio relative to the transcript level of the wild type at 0 h. Bars with different letters indicate significance at P < 0.01 by two-way ANOVA and the Tukey's honestly significant difference test (Supplemental Figure 9).

(B) Transcriptional activation by ARR1 via the *CRF2* promoter in Arabidopsis protoplasts. The values on the *y* axis represent the relative light units of LUC activity after normalizing to GUS activity. Mean ± se values determined from *n* = three biological replicates (each biological replicate was estimated as the average of two technical RT-qPCR replicates). Asterisks indicate significance at P < 0.001 using Student's *t* test when compared to controls.

(C) Activation of *CRF2* expression by ARR1:GR in the presence of cycloheximide. Ten-day-old *Pro35S:ARR1ΔDDK:GR* plants were incubated with DEX, cycloheximide, or DEX and cycloheximide for 2 h under the light. Mean ± se values determined from *n* = three biological replicates (each biological replicate was estimated as the average of two technical RT-qPCR replicates). Bars with different letters indicate significant differences at P < 0.01 by one-way ANOVA with the Tukey's honestly significant difference test (Supplemental Figure 9).

(D) Schematic diagram of *CRF2*. The nucleotide sequences, 5′-AGATT-3′, to which ARR1 binds, are indicated by circles in the promoter region. The arrowhead indicates the probe region used for EMSA. P1, P2, P3, and P4 indicate the promoter regions for the ChIP assays **(F)**. The black box indicates exon. P1, −1171 ~ −1001 nucleotides from AUG; P2, −738 ~ −552; P3, −270 ~ −128; P4, −44 ~ +79.

(E) EMSA of ARR1 with a *CRF2* promoter DNA probe. EMSA was performed with 250 ng of GST:ARR1 and 400 fmol of the indicated DNA probe. In the left panel, EMSA was performed with increasing quantities of unlabeled probe A at 10-, 50-, 100-, or 200-fold relative to the quantity of radiolabeled probe A. In the right panel, EMSA was performed with increasing quantities of unlabeled probe B at 10-, 50-, 100-, or 200-fold relative to the quantity of radiolabeled

bind to probe A (Figure 3E). This binding was easily outcompeted with increasing quantities of specific probe A but was not affected by a nonspecific probe B. We also conducted chromatin immunoprecipitation (ChIP) assays using two lines of *ARR1OX/arr1-3* plants in four different regions from P1 to P4 in the *CRF2* promoter (Figure 3D) with or without cold treatment for 3 h (Figure 3F). The ChIP assay results showed that ARR1 binds to the *CRF2* chromatin primarily in the P1 and P2 regions harboring the conserved ARR1 binding sites, whereas ARR1 did not bind to the P3 and P4 regions which do not have an ARR1 binding site. However, cold treatment did not affect the binding of ARR1 to the *CRF2* chromatin. Taken together, these results demonstrated that ARR1 directly binds to the *CRF2* promoter in vitro and in vivo and that cold does not alter the binding of ARR1 to the *CRF2* chromatin.

CRF2 and *CRF3* Promote Lateral Root Formation

To determine tissue-specific expression patterns of *CRF2* and *CRF3*, we generated transgenic Arabidopsis harboring the 2-kb promoter region of *CRF2* or *CRF3* fused to a *EGFP:GUS* reporter gene and conducted histochemical GUS assays for these transgenic plants. Pro_{CRF2}:*EGFP:GUS* (*CRF2:GUS*) plants showed strong GUS expression in both the shoot and root regions, the vascular tissue of leaves and the root, mature LRs, and LRP (Figures 4A to 4E). Pro_{CRF3}:*EGFP:GUS* (*CRF3:GUS*) plants showed GUS expression patterns similar to those of Pro_{CRF2}:*EGFP:GUS* plants except for GUS expression in the reproductive organs such as the anther and stigma (Figures 4F to 4L). As we detected strong GUS expression in LRP and LR in both transgenic GUS reporter plants, GUS expression of these transgenic plants during LRP development was determined at given developmental stages based on the classification by Malamy and Benfey (1997). In the case of Pro_{CRF2}:*EGFP:GUS* plants, GUS expression was detectable at stage I LRP and increased during LRP development up to LR emergence (Figures 4M). By contrast, GUS expression in Pro_{CRF3}:*EGFP:GUS* plants was nearly undetectable at stage I LRP but gradually increased from stage III LRP up to LR emergence (Figure 4N). Relatively stronger GUS expression was detected up to stage V in Pro_{CRF2}:*EGFP:GUS* plants than in Pro_{CRF3}:*EGFP:GUS* plants. These GUS expression patterns indicated the potential role of *CRF2* and *CRF3* during LR development.

In order to investigate the biological role of *CRF2* and *CRF3*, we isolated *crf2-2*, *crf3-2*, and *crf3-3* Arabidopsis T-DNA insertion mutants and generated *crf2-2 crf3-2* and *crf2-2 crf3-3* double mutants. As shown in Supplemental Figure 3, the *crf2-2*, *crf3-2*, and *crf3-3* mutants have T-DNA insertions in exon region of *CRF2* or *CRF3* and displayed undetectable expression of *CRF2* or *CRF3* by both RT-PCR and RT-qPCR analysis, demonstrating

that these *crf* mutants are null. We also produced transgenic Arabidopsis overexpressing CRF2 or CRF3 tagged with three copies of HA epitopes (Pro_{35S}:*3xHA:CRF2* or Pro_{35S}:*3xHA:CRF3*) (Supplemental Figure 3). Analysis of the morphological changes in *crf2* and *crf3* single and double mutants and overexpression lines compared with wild-type revealed root phenotypes (Figure 5). Primary root lengths of *crf2* and *crf3* single mutants were significantly shorter than those of the wild type but were similar to those of *crf2 crf3* double mutants (Figures 5A and 5B), indicating that *CRF2* and *CRF3* are involved in primary root development through the same genetic pathway. We found that while the LR density of *crf2-2* single mutants (2.06 ± 0.40) was similar to that of the wild type (2.08 ± 0.34), those of *crf3-2* (1.61 ± 0.28) and *crf3-3* (1.67 ± 0.34) single mutants were reduced compared with that of the wild type, and those of *crf2-2 crf3-2* (1.11 ± 0.39) and *crf2-2 crf3-3* (1.27 ± 0.40) double mutants were further reduced compared with those of *crf3* single mutants (Figure 5C). The reduction in LR density of *crf3-2* mutants was significantly rescued by expressing *CRF3* under the control of the *CRF3* promoter (Supplemental Figure 4C). These results indicated that *CRF3* plays a role in LR formation and that *CRF2* acts with *CRF3* to regulate LR formation. Three different transgenic lines overexpressing *CRF2* or *CRF3* displayed a significant increase in LR density compared with that of the wild type, whereas primary root lengths were slightly reduced in all transgenic overexpression lines (Figures 5D to 5F). These results together demonstrated that both *CRF2* and *CRF3* positively regulate LR formation.

CRF2 and *CRF3* Regulate LR Initiation

To identify the steps of LR development in which *CRF2* and *CRF3* act, we enumerated LRP densities from stage I to stage VII. Although the mean LRP density at stage I of *crf2-2* mutants (0.71 ± 0.29) was insignificantly lower than that of the wild type (0.83 ± 0.16), the mean LRP densities at stage I of *crf3-3* (0.4 ± 0.2) and *crf2-2 crf3-3* (0.47 ± 0.17) mutants were significantly lower than that of the wild type (Figure 6A). We also showed that the reduction in LRP density at stage I of *crf3-2* mutants was significantly rescued by expressing *CRF3* under the control of the *CRF3* promoter (Supplemental Figure 5). Two lines of transgenic Arabidopsis overexpressing *CRF2* or *CRF3* displayed increased LRP densities at stages I and II. These results indicated that both *CRF2* and *CRF3* are involved in promoting LR initiation. As *crf2-2* mutants displayed a similar number of primordia at stage I compared with that of the wild type, and since the double mutations in *crf2* and *crf3* did not further increase a delay in LR initiation caused by *crf3* single mutation, we conducted a LR induction experiment which allows the direct analysis of LR development kinetics rather

Figure 3. (continued).

probe A. GST was used as the negative control protein for EMSA. FP, free probe. A, probe A region (−1102 ∼ −1076 nucleotides from AUG); B, probe B region (−47 ∼ −19) indicated by the arrowhead in the **(D)**.
(F) ChIP assays of ARR1 binding to the *CRF2* promoter. The *arr1-3* and *ARR1OX/arr1-3* plants grown on 0.5× MS agar plates for 13 d at 23°C were treated for 3 h at either 23°C (upper panel) or 1°C (bottom panel) before harvesting plant materials. The *ACTIN7* DNA fragment was used for normalization. Mean ± SD values were determined from three technical qPCR replicates. Number and ab indicate line number of *ARR1OX/arr1-3* transgenic plants and antibody, respectively.
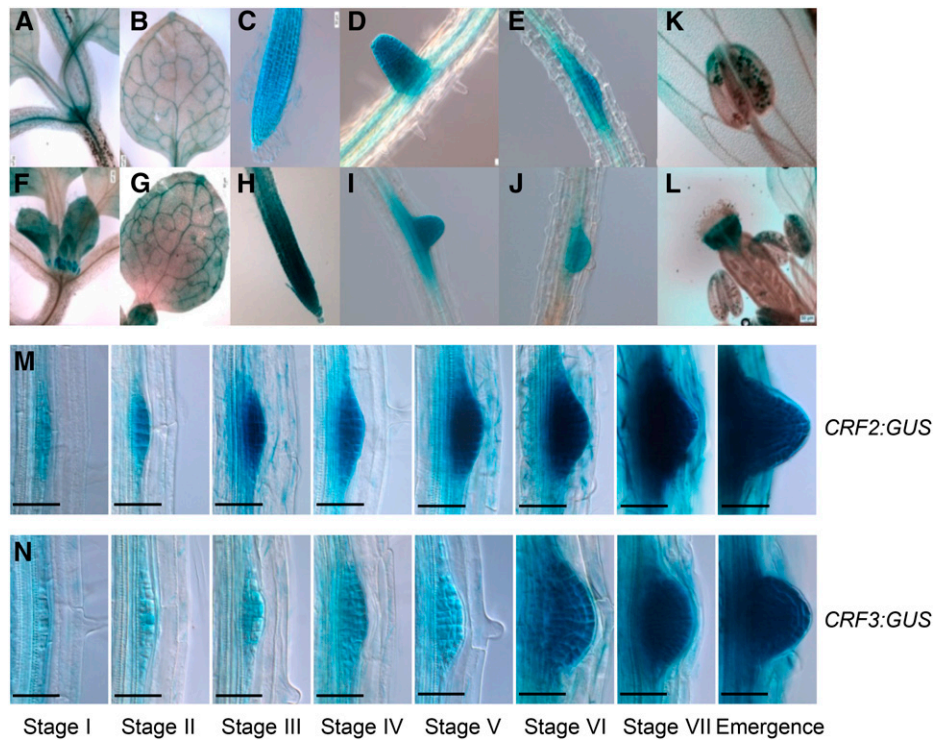
Figure 4. Analysis of Tissue-Specific Expression of *Pro*_{CRF2}:*EGFP:GUS* and *Pro*_{CRF3}:*EGFP:GUS* Transgenic Arabidopsis.

(A) to **(E)** GUS expression in the shoot apex **(A)**, leaf **(B)**, primary root **(C)**, lateral root **(D)**, and lateral root primordia **(E)** of 12-d-old *Pro*_{CRF2}:*EGFP:GUS* (*CRF2: GUS*) seedlings. Bars = 50 μm.

(F) to **(L)** GUS expression in the shoot apex **(F)**, leaf **(G)**, primary root **(H)**, lateral root **(I)**, and lateral root primordia **(J)** of 12-d-old seedlings and anthers **(K)** and a stigma **(L)** of 5-week-old *Pro*_{CRF3}:*EGFP:GUS* (*CRF3:GUS*) plants. Bars = 50 μm.

(M) and **(N)** Analysis of GUS expression in *Pro*_{CRF2}:*EGFP:GUS* **(M)** and *Pro*_{CRF3}:*EGFP:GUS* **(N)** transgenic Arabidopsis during LR development. Seven-day-old light-grown transgenic plants were incubated for 14 h with 5-bromo-chloro-3-indolyl glucuronide (X-Glu) for GUS staining. Bars = 50 μm.

than the analysis of the LRP and LRs at a given developmental stage of plants (Péret et al., 2012; Lee and Kim, 2013). We applied a gravitropic stimulus inducing initiation of LRs to the wild type, *crf* mutants, and transgenic overexpression lines grown vertically for 3 d by rotating the agar plate through 90°. We then measured the number of newly developed primordia on the convex side of the curves at 30 and 54 h postgravitropic induction (pgi) and determined the relative distribution of the LRP at stages I to VIII. Both *crf2-2* and *crf3-2* mutants showed delayed LRP development in response to the gravitropic stimuli, and *crf2-2 crf3-2* double mutants displayed more delayed LRP development compared with that of the corresponding single mutants (Figure 6B). Moreover, the *crf3-2* and *crf2-2 crf3-2* mutants displayed 20 and 35% blockage (percentage of plants with no primordium), respectively, of LR initiation events compared with that of the wild type at 30 h pgi (Figure 6B). Distribution of the LRP at stages I to VIII in the *crf2-2*, *crf3-2*, and *crf2-2 crf3-2* mutants showed that developmental transitions from stages I to III were inhibited to some extent at 30 h pgi and the LRP development of these *crf* mutants was delayed at 54 h pgi compared with that of the wild type. By contrast, overexpression of *CRF2* or *CRF3* in transgenic Arabidopsis stimulated LRP developmental processes from initiation to emergence of LRP at both 30 and 54 h pgi compared with that of

the wild type. Taken together, these results demonstrated that *CRF2* and *CRF3* positively control LR initiation in different genetic pathways and that *crf3* exhibits a stronger genetic effect on LR development than does *crf2*.

CRF2 and *CRF3* Are Required for LR Initiation under Cold Stress

As *CRF2* and *CRF3* respond to cold (Figure 1) and play a role during LR initiation and LR development (Figures 5 and 6), we sought to characterize the role of *CRF2* and *CRF3* during LR development when plants are exposed to cold temperatures. We first determined cold response of *CRF2* and *CRF3* during LRP development and in LRs using GUS reporter transgenic plants. Cold treatment for 8 h enhanced GUS expression in LRP from stage III to the emerged LRs and elongated LRs of both *Pro*_{CRF2}:*EGFP:GUS* and *Pro*_{CRF3}:*EGFP:GUS* plants (Figures 7A and 7B). Cold also enhanced GUS staining in leaves of both *Pro*_{CRF2}:*EGFP:GUS* and *Pro*_{CRF3}:*EGFP:GUS* seedlings (Supplemental Figure 6), which is consistent with the RT-qPCR data (Figure 1C).

As *CRF2* and *CRF3* respond to cold during LRP development and play a role in LR initiation, we investigated whether *CRF2* and
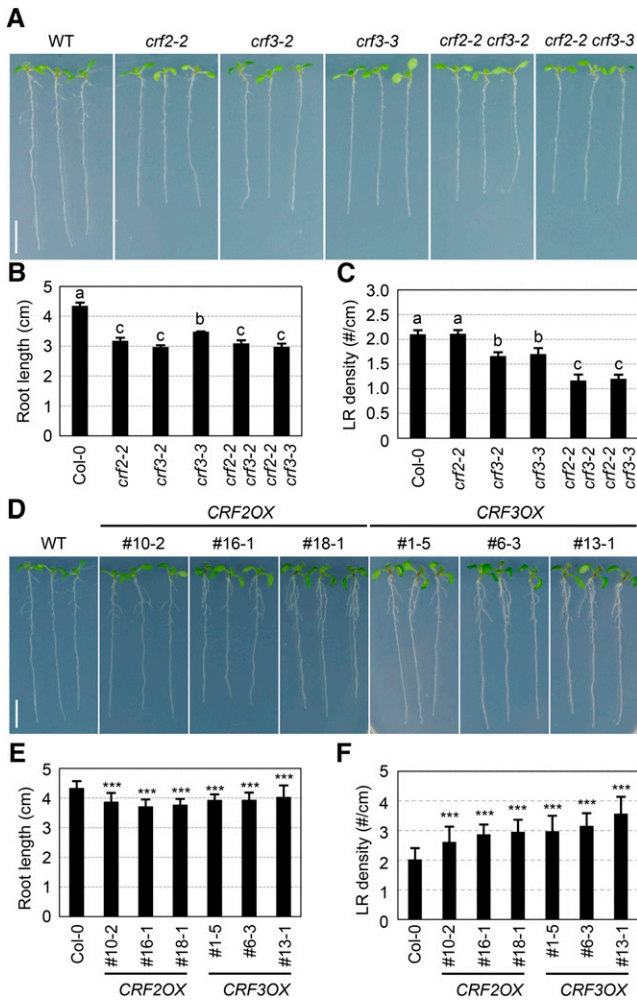
Figure 5. Root Lengths and LR Densities of the Wild Type, *crf2-2*, *crf3-2*, *crf3-3*, *crf2-2 crf3-2*, *crf2-2 crf3-3* Mutants, and *Pro_{35S}:3xHA:CRF2* and *Pro_{35S}:3xHA:CRF3* Transgenic Arabidopsis.

(A) Representative seedlings of the wild-type, *crf2-2*, *crf3-2*, *crf3-3*, *crf2-2 crf3-2*, and *crf2-2 crf3-3* mutants. Plants were grown vertically for 8 d. Bars = 1 cm.

(B) Root lengths of wild-type, *crf2-2*, *crf3-2*, *crf3-3*, *crf2-2 crf3-2*, and *crf2-2 crf3-3* mutants. Plants were grown vertically for 8 d and root lengths were measured. Mean ± SD values were determined from three biological replicates of 28 seedlings. Bars with different letters indicate significant differences at P < 0.05 by one-way ANOVA with the Tukey's honestly significant difference test (Supplemental Figure 9).

(C) LR densities of wild-type, *crf2-2*, *crf3-2*, *crf3-3*, *crf2-2 crf3-2*, and *crf2-2 crf3-3* mutants. LR numbers (#) per unit primary root length (cm) measured from plants grown vertically for 8 d were plotted. Mean ± SD values were determined from three biological replicates of 28 seedlings. Bars with different letters indicate significant differences at P < 0.01 by one-way ANOVA with the Tukey's honestly significant difference test (Supplemental Figure 9).

(D) Representative seedlings of wild-type, *Pro_{35S}:3xHA:CRF2* (*CRF2OX*), and *Pro_{35S}:3xHA:CRF3* (*CRF3OX*) transgenic plants. Plants were grown vertically for 8 d. Bars = 1 cm.

(E) Root lengths of wild-type, *Pro_{35S}:3xHA:CRF2*, and *Pro_{35S}:3xHA:CRF3* transgenic plants. Plants were analyzed as described in the Figure 5B

CRF3 are required for LR initiation when plants are exposed to cold stress. To this end, 3-d-old wild-type, *crf2-2*, *crf3-2*, *crf2-2 crf3-2*, *Pro_{35S}:3xHA:CRF2*, and *Pro_{35S}:3xHA:CRF3* plants were subjected to a 90° gravitropic stimulus and treated for 8, 10, or 12 h at 4°C and then placed back to 23°C while being subjected to a 90° gravitropic stimulus, and LR initiation events were then measured at 30 h pgi (Figure 7C). To detect significant differences between genotypes and treatments with their respective controls, we first used two-way ANOVA, combining different cold treatment incubation times with different genotypes, but this did not capture significant differences, due to the amount of intrinsic variation in LR development between genotypes. As an alternative statistical analysis, we conducted one-way ANOVA to capture significant differences among the different incubation times for cold treatment in a given genotype as indicated by bars with different capital letters or with primed different capital letters and then conducted another one-way ANOVA to capture significant differences among different genotypes for the given cold treatment time as indicated by bars with different small letters or with primed different small letters. The results showed that LR initiation events in the wild type decreased with increasing time of cold treatment at 4°C and that *crf2-2* mutants exhibited a further decrease in LR initiation events compared with those of the wild type. The effects of cold stress on the LR initiation events of *crf3-2* mutants were more severe than those of *crf2-2* mutants. The *crf2-2 crf3-2* double mutants exposed to cold stress displayed additively reduced LR initiation events compared with those of the corresponding *crf* single mutants. Overexpression of *CRF2* or *CRF3* in transgenic Arabidopsis prevented the decrease in LR initiation events caused by cold stress to some extent compared with the wild type (right panel of Figure 7C). We further showed that reduction in LR initiation events of *crf2-2* or *crf3-2* mutants under cold stress was significantly rescued by expressing *CRF2* or *CRF3* under the control of their own promoter in the corresponding mutants (Figure 7D). These results suggested that *CRF2* and *CRF3* are necessary for LR initiation via different genetic pathways when plants are exposed to cold stress.

DISCUSSION

As LRs are the major determinant of the root system architecture in plants, the developmental plasticity of LR formation is important for the survival of plants to continually changing environmental conditions. In Arabidopsis, the developmental and molecular mechanisms of LR formation have been well characterized (Lavenus et al., 2013) and the genetic pathways regulating LR branching in response to environmental cues such as nutrients including nitrate and phosphate, salt, and gravity have been

legend. Mean ± SD values were determined from 30 seedlings. Asterisks indicate significant differences at P < 0.001 using Student's *t* test when comparing to the wild type.

(F) LR densities of wild-type, *Pro_{35S}:3xHA:CRF2*, and *Pro_{35S}:3xHA:CRF3* transgenic plants. Plants were analyzed as described in the Figure 5C legend. Mean ± SD values were determined from 30 seedlings. Asterisks indicate significant differences at P < 0.001 using Student's *t* test compared to the wild type.
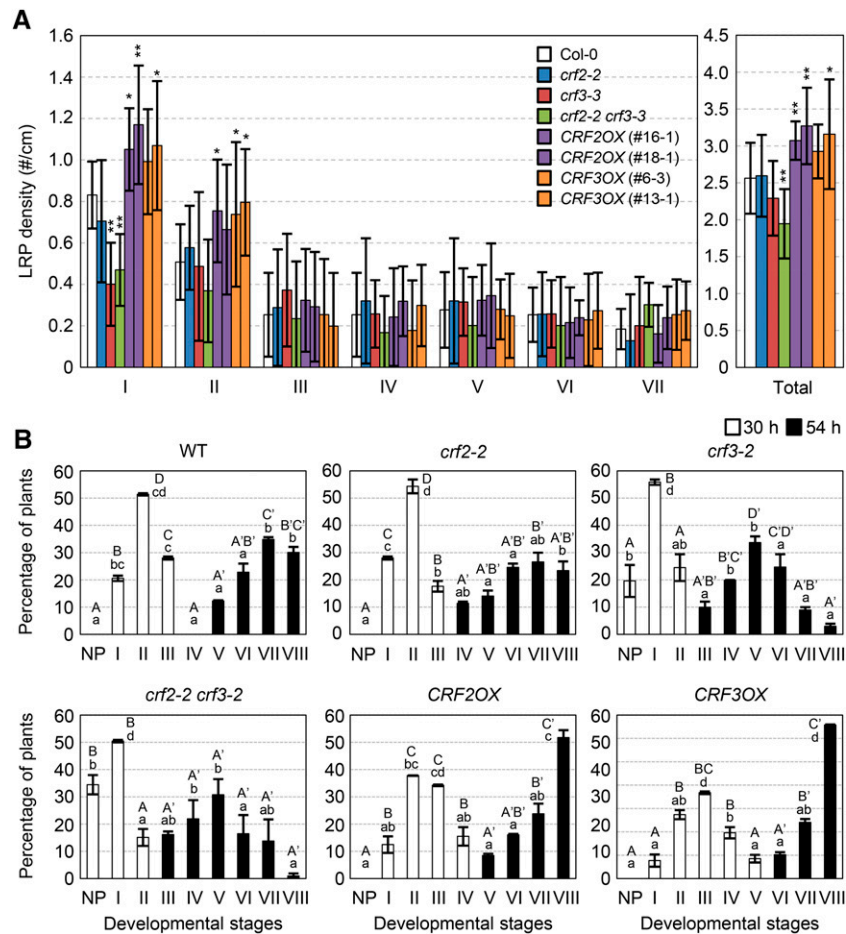
Figure 6. Analysis of LR Developmental Kinetics in *crf2*, *crf3*, and *crf2 crf3* Mutants and *Pro₃₅ₛ:3xHA:CRF2* and *Pro₃₅ₛ:3xHA:CRF3* Transgenic Arabidopsis.

(A) LR primordia densities of wild-type, *crf2-2*, *crf3-3*, and *crf2-2 crf3-3* mutants and *Pro₃₅ₛ:3xHA:CRF2* and *Pro₃₅ₛ:3xHA:CRF3* transgenic plants at given developmental stages. Plants were grown vertically for 8 d and the numbers of LR primordia per root length (#/cm) were measured at given developmental stages before the emergence of LRs. Mean ± SD values were determined from 10 seedlings. Asterisks indicate significant differences using Student's *t* test when compared to the wild type (*P < 0.05; **P < 0.01).

(B) LR developmental kinetics of wild-type, *crf2-2*, *crf3-2*, and *crf2-2 crf3-2* mutants and *Pro₃₅ₛ:3xHA:CRF2* and *Pro₃₅ₛ:3xHA:CRF3* plants after synchronization with a gravitropic stimulus. Three-day-old plants were subjected to a 90° gravitropic stimulus, and the numbers of LR primordia at stages I-VIII were determined at 30 h pgi (white bars) and 54 h pgi (black bars). Mean ± SD values were determined from two biological replicates of 50 seedlings. Bars with different capital letters or with primed different capital letters indicate significant differences among different stages at 30 and 54 h pgi in the given genotype by one-way ANOVA with the Tukey's honestly significant difference test at P < 0.05, respectively. Bars with different small letters indicate significant differences among different genotypes at the given same stage by one-way ANOVA with the Tukey's honestly significant difference test at P < 0.05 (Supplemental Figure 9). NP, no primordium.

identified (Dastidar et al., 2012; Tian et al., 2014). While cold is one of the critical environmental conditions that limits plant growth and development as well as crop yield (Jeon and Kim, 2013), it is not known how genetic components are involved in LR adaptation response to cold. This study demonstrated that *CRF2* and *CRF3* play an important role during LR development in Arabidopsis and also integrate the cold signal into LR development for an adaptation response to cold stress via signaling pathways as depicted in the model (Figure 8). A recent study showed that CRF2 and CRF6 transcriptionally control genes encoding PIN-FORMED (PIN) auxin transporters such as *PIN1* and *PIN7*, providing a crosstalk component that fine-tunes auxin transport capacity

downstream of cytokinin signaling to control plant growth and development (Šimášková et al., 2015). Therefore, *CRF2* and *CRF3* gate endogenous hormone signals, such as cytokinin and auxin, as well as the environmental cold signal, providing adaptation versatility to the plants under cold stress. It remains to be determined whether *CRF2* promotes LR initiation under cold stress through upregulation of *PIN* gene expression.

This work showed that a subset of the cytokinin TCS system is utilized for cold signaling to express *CRF2*. A significant change in cold-responsive expression of *CRF2* in *ahk2 ahk3* double mutants was detected (Figure 2A), indicating that *AHK4* may be involved in the cold response of *CRF2* in addition to *AHK2* and *AHK3*.
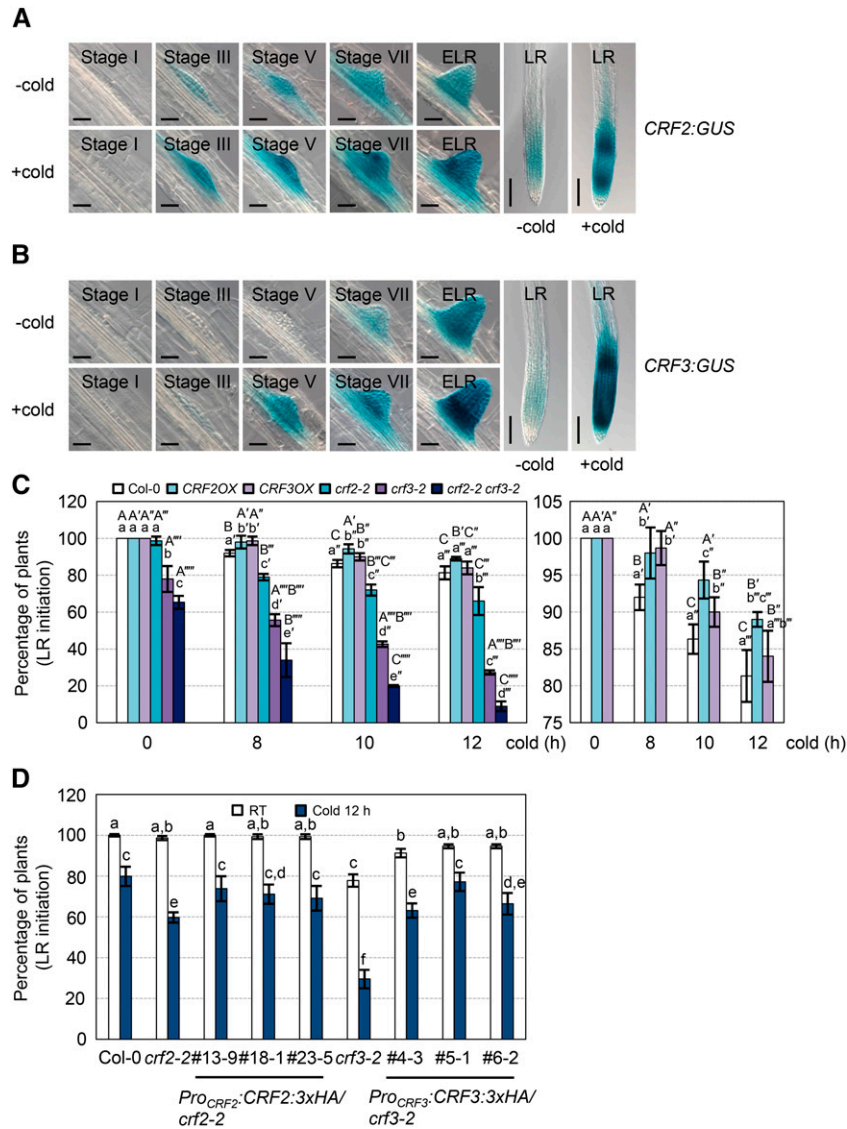
Figure 7. Effect of Cold Stress on GUS Expression and LR Initiation Events.

(A) and **(B)** GUS expression in LR primordia of 7-d-old light-grown Pro_{CRF2}:*GUS* plants **(A)** and Pro_{CRF3}:*GUS* plants **(B)** at 23°C (−cold) or treated for 8 h at 1°C (+cold). Plants were incubated for 14 h with X-Glu for GUS staining. Bars = 50 μm.

(C) Analysis of cold stress on LR initiation events of Col-0, Pro_{35S}:*3xHA:CRF2* (*CRF2OX*), and Pro_{35S}:*3xHA:CRF3* (*CRF3OX*) transgenic lines and *crf2-2*, *crf3-2*, *crf2-2 crf3-2* mutants after synchronization with a gravitropic stimulus. Three-day-old plants were subjected to a 90° gravitropic stimulus and treated for 8, 10, or 12 h at 4°C, and the LR initiation events from these plants were then determined at 30 h pgi. Mean ± SD values were determined from three biological replicates of 50 seedlings per replicate. Bars with different capital letters or with primed different capital letters indicate significant differences at P < 0.05 among the different incubation times for cold treatment in the given genotype by one-way ANOVA with the Tukey's honestly significant difference test. Bars with different small letters or with primed different small letters indicate significant differences at P < 0.05 among different genotypes for the given cold treatment time by one-way ANOVA with the Tukey's honestly significant difference test (Supplemental Figure 9).

(D) Analysis of cold stress on LR initiation events of Pro_{CRF2}:*CRF2:3xHA/crf2-2* and Pro_{CRF3}:*CRF3:3xHA/crf3-2* transgenic Arabidopsis compared with Col-0, *crf2-2*, and *crf3-2*, after synchronization with a gravitropic stimulus. Assays were conducted as described in the Figure 7C legend. Mean ± SD values were determined from three biological replicates of 50 seedlings. Bars with different letters indicate significant differences at P < 0.05 by two-way ANOVA and the Tukey's honestly significant difference test (Supplemental Figure 9). RT = 23°C.

However, *ahp1,2,3,4,5* pentuple mutants also exhibited significant levels of *CRF2* expression in response to cold (Figure 2B), suggesting that an additional gene regulatory pathway other than the TCS pathway is involved in cold response of *CRF2*. None of the

TCS mutants used in this study affected cold-responsive expression of *CRF3* (Figure 2), showing that the cold response of *CRF3* occurs independently of the TCS system. A microarray analysis conducted on the Arabidopsis mutant harboring
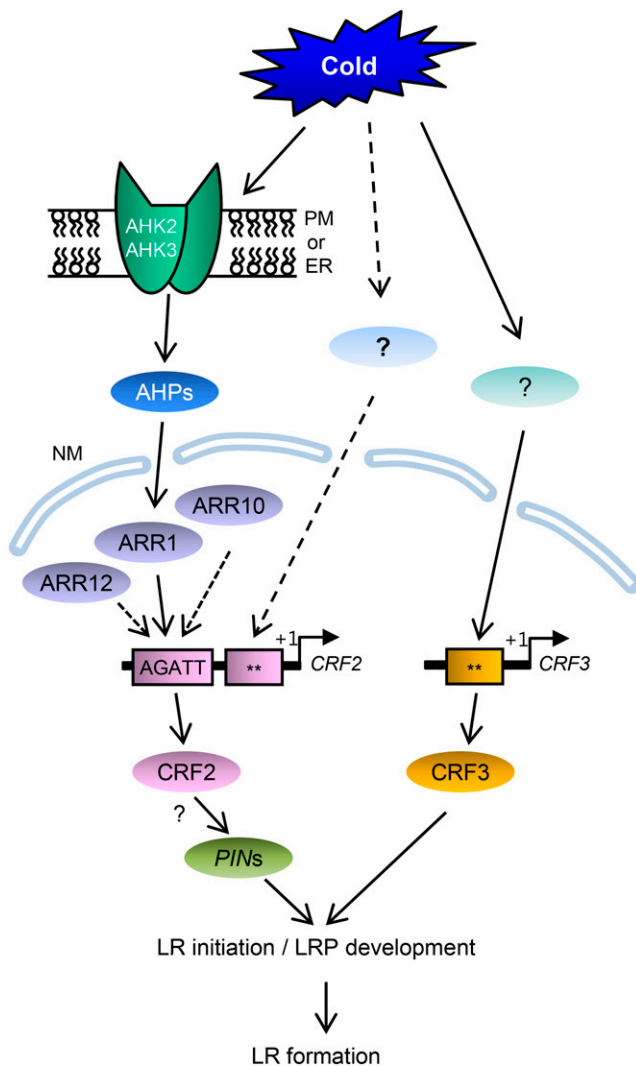
Figure 8. Model Showing *CRF2* and *CRF3*-Mediated Lateral Root Formation in Arabidopsis under Cold Stress.

Regulation of *PIN*s by CRF2 has been reported recently (Šimášková et al., 2015). Solid arrows indicate positive regulation. Dotted arrows indicate putative signaling pathways. Double asterisks indicate unknown *cis*-elements. ER, endoplasmic reticulum; NM, nuclear membrane; PM, plasma membrane.

a dominant mutation in *INDUCER OF C-REPEAT/DEHYDRATION RESPONSE ELEMENT BINDING FACTOR EXPRESSION1* (*ice1*) indicated that *CRF3* may be regulated by *ICE1* (Lee et al., 2005). However, our analysis with loss-of-function mutants *ice1* and *ice2* (Fursova et al., 2009) showed that these mutations only slightly affected cold-responsive expression of *CRF3* (Supplemental Figure 7), suggesting that a gene regulatory network other than *ICE1* may be involved in cold response of *CRF3*.

arr1,10,12 triple mutations reduced cold-responsive expression of *CRF2* by 60% compared with that in the wild type (Figure 2C), indicating that ARR1, ARR10, and ARR12 are the main transcription factors regulating the cold response of *CRF2*. To identify if

these type-B ARRs directly regulate *CRF2* expression in response to cold, we used a variety of molecular approaches such as transient gene expression assays, DEX-inducible nuclear translocation of GR-fused CRF2, EMSA, and ChIP assays (Figure 3), demonstrating that ARR1 directly regulates *CRF2* expression by binding to the *CRF2* promoter. The ChIP assay results demonstrated that cold did not enhance the ARR1 binding to the *CRF2* promoter in the chromatin (Figure 3F), indicating that cold does not alter the DNA binding activity of ARR1 in vivo but rather activates the transactivation potential of ARR1. It will be interesting to determine whether the phosphorelay from AHKs via AHPs in response to cold controls the transcriptional activities of ARR1 and other type-B ARRs. SELEX and EMSA experiments have shown that ARR1, ARR2, and ARR11 bind to the same or a very similar nucleotide sequence motif, $5'$-(A/G)GAT(T/C)-$3'$ (Sakai et al., 2000; Hosoda et al., 2002; Imamura et al., 2003). Experiments using protein binding microarrays have shown that ARR11 and ARR14 preferentially bind to $5'$-AGATACG-$3'$ or $5'$-AGATCTT-$3'$ or similar sequences (Franco-Zorrilla et al., 2014). Thus, ARR10 and ARR12 or other type-B ARRs may directly promote *CRF2* expression through binding to the core cytokinin response motif sequence that resides in the *CRF2* promoter region.

Analysis of a variety of root transcript profiling data sets showed that a set of 1920 genes display transcriptional changes in the xylem pole pericycle cells during lateral root initiation (Swarup et al., 2008). This set of genes included *CRF2* but not *CRF3* (Swarup et al., 2008). Our GUS expression analysis of *ProCRF2: EGFP:GUS* plants showed variable staining of GUS at stage I LRP, probably due to low and/or dynamic expression, as shown in Figures 4M and 7A. Variable expression of GUS at stage III LRP in *ProCRF3:EGFP:GUS* plants was also noted (Figures 4M and 7B). These results may be due to the stochastic nature of *CRF2* and *CRF3* expression. Relatively large variations in LRP densities were noticed in this study (Figure 6A) as well as in the report by Swarup et al. (2008). Stochastic fluctuations in gene expression have been proposed to underlie the phenotypic variation and cellular variation in eukaryotic organisms even in fixed genetic and environmental contexts (Blake et al., 2003; Raj et al., 2010). Such stochastic effects in gene expression could have implications in LR development, as they might generate variation in the distribution of LRP at a variety of different developmental stages.

Analysis of the expression profiling of *CRF*s in response to various plant hormones and in a variety of mutant backgrounds using the Genevestigator Web tool showed that *CRF2* weakly responds to auxin but strongly responds to cytokinins and is unresponsive to cytokinins in *ahk2 ahk3* mutants (Figure 1A; Supplemental Figure 8), indicating that cytokinin may regulate *CRF2* expression through the AHK2- and AHK3-mediated TCS pathway. However, cytokinins are known to negatively control LR formation by preventing the establishment of an auxin gradient required for LR formation and to act as a paracrine signal regulating LR spacing (Riefler et al., 2006; Laplaze et al., 2007; Bielach et al., 2012; Chang et al., 2015). Although the role of *CRF2* during the inhibitory action of cytokinin for LR formation remains to be determined, it is plausible to hypothesize that cold activates a subset of the TCS pathway to express *CRF2*. *CRF3* responds to auxin and is unresponsive to auxin in *arf7*, *arf19*, and *arf7 arf19* mutant backgrounds (Figure 1A; Supplemental Figure 8),

suggesting that auxin may regulate *CRF3* expression through ARF7 and ARF19. The previous studies showed that cold temperature inhibits root basipetal auxin transport and reduces auxin accumulation, limiting root growth in Arabidopsis (Shibasaki et al., 2009; Zhu et al., 2015), indicating that cold temperature inhibits auxin transport, biosynthesis, and response in the root. We speculate that the expression of *CRF2* and *CRF3* in response to cold may be an adaptation mechanism of plants under cold stress, enabling LR initiation and development to overcome the auxin-mediated cold-induced inhibition of root growth, thus influencing changes in root system architecture in response to cold.

Several transcription factors, including LATERAL ORGAN BOUNDARIES DOMAIN/ASYMEMETRIC LEAVES2-LIKE (LBD/ASL) proteins such as LBD16, LBD18, LBD29, and LBD33, are regulated at the transcriptional level downstream of Aux/IAA-ARF modules in response to auxin to control LR development (Okushima et al., 2007; Lee et al., 2009a, 2009b; Berckmans et al., 2011; Goh et al., 2012; Kang et al., 2013; Lee and Kim, 2013; Lee et al., 2013, 2015). Most single or double *lbd* mutations or mutations in other transcription factor genes involved in LR development downstream of *ARF*s identified thus far have not been associated with a significant reduction in LR initiation, except for *GATA23*, which is involved in the specification of the LR founder cell identity (De Rybel et al., 2010). However, the *crf3* single gene mutation caused a delay in LR initiation (Figure 6), indicating that *CRF3* may play a unique role during LR initiation.

A recent study showed that *CRF4* is induced by cold and involved in freezing tolerance (Zwack et al., 2016). *crf1,3,5,6* quadruple mutants displayed strong inhibition of primary root elongation compared with that of the wild type (Raines et al., 2016). LR numbers of both *crf2,5,6* and *crf3,5,6* triple mutants were reduced compared with the wild type (Raines et al., 2016). Loss-of-function mutations in *CRF2* or *CRF3* or both *CRF3* and *CRF6* or *CRF2*, *CRF3*, and *CRF6* caused reductions in root length, root meristem size, and LRP density, whereas overexpression of *CRF2* or *CRF3* or *CRF6* enhanced LRP density (Šimášková et al., 2015). In addition, multiple mutations in *CRF*s result in larger rosettes, delayed leaf senescence, and shorter hypocotyls in etiolated seedlings (Raines et al., 2016). These recent studies along with our present results indicate that the *CRF* genes play roles in regulating multiple aspects of plant growth and development including root system architecture and plant response to cold and freezing stress.

METHODS

Plant Materials and Growth Conditions

Wild-type and mutant lines of *Arabidopsis thaliana* were in the Columbia (Col-0) ecotype except for *ahp1-1* in the Wassilewskija (Ws) ecotype. Plants were grown on 0.5× MS agar plates or in soil at 23°C with a 16-h photoperiod. The light intensity was ~120 μmol m^{-2} s^{-1}. The *crf2-2* (SAIL371_D04), *crf3-2* (SAIL325_H03), and *crf3-3* (SALK_138253) mutants were obtained from the ABRC. The homozygous T-DNA insertion mutant lines were identified by PCR using the primers shown in Supplemental Table 1. The *crf2-2 crf3-2* and *crf2-2 crf3-3* double mutants were generated by crossing *crf2-2* (male) with *crf3-2* or *crf3-3* (female), and the resultant isolated homozygous lines were verified by PCR. The null mutations of *crf2-2*, *crf3-2*, *crf3-3*, *crf2-2 crf3-2*, and *crf2-2 crf3-3* were further verified by RT-PCR and RT-qPCR analysis. The *ahk2-2 ahk3-3*, *ahp2-1 ahp3 ahp5-2*,

arr1-3, *arr10-5*, *arr12-1*, *arr1-3 arr10-5*, *arr1-3 arr12-1*, *arr10-5 arr12-1*, and *arr1-3 arr10-5 arr12-1* mutants have been described previously (Jeon and Kim, 2013). *ahp1-1,2-1,3,4* was crossed to *ahp2-1,3,5-2* to generate *ahp1-1,2-1,3,4,5-2* quintuple mutants. To generate transgenic plants over-expressing the *CRF2* and *CRF3* genes, the full-length *CRF2* and *CRF3* coding regions were isolated by PCR from Arabidopsis cDNA and inserted into pDONR™221 (Invitrogen) using the Gateway BP Clonase II enzyme mix (Invitrogen) to yield pDONR221:*CRF2* and pDONR221:*CRF3*, respectively. These constructs were inserted into pGWB515 vector (Nakagawa, Shimane University, Japan) using the Gateway LR Clonase II enzyme mix (Invitrogen), yielding the *Pro$_{35S}$:3xHA:CRF2* and *Pro$_{35S}$:3xHA:CRF3* constructs, respectively. The *Pro$_{35S}$:3xHA:CRF2* and *Pro$_{35S}$:3xHA:CRF3* constructs were introduced into Arabidopsis using the vacuum infiltration *Agrobacterium tumefaciens*-mediated transformation method, and T3 homozygous transgenic plants were obtained. To generate the promoter-GUS transgenic Arabidopsis, the promoter region of *CRF2* encompassing −2005 to −1 bp relative to the AUG initiation codon and the promoter region of *CRF3* encompassing −2021 to −1 bp relative to the AUG initiation codon were isolated by PCR from Arabidopsis genomic DNA and inserted into pDONR 221 (Invitrogen) using the Gateway BP Clonase II enzyme mix (Invitrogen) to yield pDONR221:*Pro$_{CRF2}$* and pDONR221:*Pro$_{CRF3}$*, respectively. These constructs were inserted into the pBGWFS7 vector using the Gateway LR Clonase II enzyme mix (Invitrogen), yielding *Pro$_{CRF2}$:GFP:GUS* and *Pro$_{CRF3}$:GFP:GUS*, respectively. The *Pro$_{CRF2}$:GFP:GUS* and *Pro$_{CRF3}$:GFP:GUS* constructs were transformed into Arabidopsis, and T3 homozygous transgenic plants were obtained. To generate *Pro$_{CRF2}$:CRF2:3xHA/crf2-2* or *Pro$_{CRF3}$:CRF3:3xHA/crf3-3* Arabidopsis, we isolated the *CRF2* genomic DNA fragment encompassing from −2005 to +1032 bp relative to AUG initiation codon that includes the promoter and the full-length *CRF2* coding region and the *CRF3* genomic DNA fragment encompassing from −2021 to +1065 bp region that includes the promoter and the full-length *CRF3* coding region from the Arabidopsis genomic DNA by PCR using *Pfu* polymerase (Stratagene). These PCR products were then inserted into pDONR221 (Invitrogen) by BP recombination reaction using Gateway BP Clonase II Enzyme mix (Invitrogen) and subcloned into the pGWB513 vector (Nakagawa, Shimane University, Japan) by LR recombination reaction, yielding the *Pro$_{CRF2}$:CRF2:3xHA* and *Pro$_{CRF3}$:CRF3:3xHA* plasmids. These constructs were then transformed into *crf2-2* or *crf3-2* mutants by Agrobacterium-mediated transformation, and T3 homozygous transgenic mutant plants were obtained. To generate *Pro$_{35S}$:10xMYC:ARR1/arr1-3* transgenic Arabidopsis plants, the full-length *ARR1* coding regions were amplified by PCR using *Pfu* polymerase (Stratagene) and inserted into pDONR221 (Invitrogen) by BP recombination reaction using Gateway BP Clonase II Enzyme mix (Invitrogen). This construct was subcloned into the pGWB521 vector (Nakagawa, Shimane University, Japan) by LR recombination reaction, yielding *Pro$_{35S}$:10xMYC:ARR1*. This construct was transformed into *arr1-3* mutants by Agrobacterium-mediated transformation, and T3 homozygous transgenic mutant plants were obtained. All constructs were confirmed via DNA sequencing prior to plant transformation. The *35S:ARR1ΔDDK:GR* construct was generously provided by Takashi Aoyama (Sakai et al., 2000) and confirmed via genotyping prior to usage. Oligonucleotides and PCR conditions are provided in Supplemental Table 1.

RNA Isolation, RT-PCR, and RT-qPCR

The Arabidopsis plants were immediately frozen in liquid nitrogen following treatment and stored at −80°C. Total RNA was isolated from frozen Arabidopsis samples using TRI reagent (Molecular Research Center). RT-PCR analysis was performed using Access RT-PCR system (Promega) according to the manufacturer's instructions. For RT-qPCR analysis, RNA was isolated using an RNeasy Plant Mini kit (Qiagen) and the real-time RT-PCR analysis was conducted using a QuantiTect SYBR Green RT-PCR kit (Qiagen) in a CFX96TM real-time PCR detection system (Bio-Rad). Data

analysis and determination of reaction specificities were performed as described previously (Jeon et al., 2010). All real-time RT-PCR assays were conducted in duplicate for the same RNA isolated from each biological experiment. RT-qPCR analysis was performed for three different biological experiments and subjected to statistical analysis. Statistics were performed with SPSS21. Oligonucleotides and PCR conditions are provided in Supplemental Table 1.

Histochemical GUS Assays and Microscopy

Histochemical assays for GUS activity were performed with 5-bromo-4-chloro-3-indolyl glucuronide, as described previously (Jefferson and Wilson, 1991). For whole-mount visualization, the seedlings were cleared in 100% (v/v) ethanol for 24 h, and then mounted in 90% (v/v) glycerol. Samples were observed under a Leica DM2500 microscope at 50-, 200-, or 400-fold magnification with differential interference contrast or with a Nikon D300 Camera.

Transient Gene Expression Assays with Arabidopsis Protoplasts

In order to construct $Pro_{35S}{:}\Omega{:}4xHA{:}ARR1$ and $Pro_{35S}{:}\Omega{:}3xHA{:}EGFP$ effector plasmids, $ARR1$ or $EGFP$ full-length DNA was first amplified by PCR using the Pfu DNA polymerase and inserted into the $Pro_{35S}{:}GUS$ plasmid at SpeI (N terminus) and SacI (C terminus) sites in place of the GUS DNA fragment, yielding the $Pro_{35S}{:}ARR1$ or $Pro_{35S}{:}EGFP$ DNA construct. A translational enhancer sequence (Ω) from the $DR5(7X){:}\Omega{:}GUS$ plasmid was then inserted into the $Pro_{35S}{:}HA(4X){:}ARR1$ or the $Pro_{35S}\ HA(3X){:}EGFP$ construct at BamHI (N terminus) and SpeI (C terminus) sites upstream of the translation initiation site, yielding the $Pro_{35S}{:}\Omega{:}HA(4X){:}ARR1$ or the $Pro_{35S}{:}\Omega{:}HA(3X){:}EGFP$ DNA construct. Reporter plasmid was constructed by replacing GUS of $Gal4(3X){:}GUS$ vector (Tiwari et al., 2003) with the LUC DNA fragment. The $Pro_{CRF2}{:}LUC$ reporter construct was generated by replacing the Gal4(3X) DNA fragment of the $Gal4(3X){:}LUC$ plasmid (Kang et al., 2013) with the $CRF2$ promoter encompassing the nucleotides from -2005 to -1 bp relative to the AUG initiation codon. These promoter regions were amplified by PCR from the genomic DNA of Arabidopsis Col-0 with primers harboring PstI site at the 5′-end and SpeI site at the 3′-end. The $35S{:}GUS$ vector was used as a transfection control (Lee et al., 2008). All the constructs were verified by DNA sequencing. The plasmids were purified using a Qiagen Plasmid Midi kit prior to protoplast transfection. Protoplasts were isolated from rosette leaves of 2- to 3-week-old Arabidopsis plants on an MS plate under a 16-h photoperiod, transfected with plasmid DNA, and incubated for 18 h in the dark at room temperature, as described previously (Lee et al., 2008). Total proteins were extracted using $1\times$ Passive Lysis buffer (Promega) according to the manufacturer's protocol. LUC activity was then determined using the Dual-Luciferase Reporter Assay System (Promega) with the Synergy H1 Hybrid Multi-Mode Microplate Reader (BIO-TEK Instruments). GUS activity was assayed with 1 mM 4-methylumberlliferyl-β-D-glucuronide in GUS extraction buffer as described previously (Ulmasov et al., 1997). After terminating the reaction with 0.2 M Na_2CO_3, the appearance of the GUS reaction product MU was measured with the Synergy H1 Hybrid Multi-Mode Microplate Reader (BIO-TEK Instruments). LUC activity was normalized to the GUS activity. Transfection was performed in triplicate. Duplicate LUC and GUS assays were performed for each transfection. Oligonucleotides and PCR conditions are provided in Supplemental Table 1. Statistics were performed with SPSS21 using Student's t test.

Preparation of the Recombinant Proteins

The $ARR1$ cDNA region coding for the DNA binding domain (1 to 300 amino acids) was amplified by PCR with gene-specific primers and inserted into the pGEX 4T-1 vector at BamHI (N terminus) and XmaI (C terminus) sites, yielding the $GST{:}ARR1$ plasmid. The recombinant proteins were produced in bacterial strain BL21-CodonPlus(DE3)-RIL cells (Stratagene) by inducing the expression of recombinant proteins at 25°C overnight with 0.2 mM isopropyl-1-thio-β-D-galactopyranoside in a shaking incubator. The cultured bacterial cells were lysed with $1\times$ PBS buffer by sonication with the Vibra-Cell VCX130 (Sonics and Materials). The GST-fusion proteins were purified using glutathione-Sepharose 4B (GE Healthcare), according to the manufacturer's instructions. The purified proteins were then dialyzed against the binding buffer (40 mM Tris-HCl, pH 7.5, 100 mM KCl, 0.2 mM EDTA, 0.5 mM DTT, and 25% glycerol). Oligonucleotides and PCR conditions are provided in Supplemental Table 1.

EMSA

The EMSA was conducted essentially as described previously (Lee et al., 2013). To prepare DNA probes for EMSA, the oligonucleotides (29-mers) were denatured by boiling them for 5 min, followed by slow cooling to 23°C. The annealed oligonucleotides were radiolabeled with [α-^{32}P]dCTP by the standard Klenow fill-in reactions and then purified on G-50 micro columns (GE Healthcare), according to the manufacturer's instructions. The binding reaction was performed in 10 μL of reaction mixture containing 400 fmol DNA probes, binding buffer (20 mM HEPES KOH, pH 7.6, 80 mM KCl, 1 mM DTT, and 10% glycerol), 200 ng of poly(dI-dC), 4 μg of BSA, and 250 ng of the purified GST fusion proteins at room temperature for 30 min. The samples were then analyzed by 4.5% native polyacrylamide gel electrophoresis. Sequences for the DNA probes used in EMSA are provided in Supplemental Table 2.

ChIP Assays

The ChIP assays were conducted essentially as described previously (Jeon and Kim, 2011). Fifteen-day-old seedlings were treated with or without cold for 3 h. DNA from these seedlings was immunoprecipitated with an anti-c-Myc agarose affinity gel antibody (Sigma-Aldrich). Quantitative PCR analysis was conducted using SsoFast EvaGreen Supermix (Bio-Rad) on a CRF96 real-time system machine (Bio-Rad). The PCR primers for qPCR were designed to amplify the DNA fragments of 100 to 200 bp and are shown in Supplemental Table 1. The $ACTIN7$ DNA fragment was used for normalization.

Phenotypic Analysis

Phenotypic analysis was conducted as described previously (Park et al., 2002). Root lengths were measured from scans of the roots using the ImageJ software (Media Cybernetics). The numbers of LRs and LRP were scored using a Leica DM2500 microscope according to Malamy and Benfey (1997). LR induction experiments were conducted as described previously (Lee and Kim, 2013). Three-day-old seedlings were subjected to a 90° gravitropic stimulus, and the numbers of LRP at stages I-VIII (emerged) were determined at 30 and 54 h pgi. Statistics were performed with SPSS21, using Student's t test or ANOVA with Tukey's honestly significant difference test post-hoc analyses.

Accession Numbers

Sequence data from this article can be found in the Arabidopsis Genome Initiative or GenBank/EMBL database under the following accession numbers: $CBF1$ (At4g25490), $CRF2$ (At4g23750), $CRF3$ (At5g53290), $AHK2$ (At5g35750), $AHK3$ (At1g27320), $AHP1$ (At3g21510), $AHP2$ (At3g29350), $AHP3$ (At5g39340), $AHP4$ (At3g16360), $AHP5$ (At1g03430), $ARR1$ (At3g16857), $ARR10$ (At4g31920), $ARR12$ (At2g25180), $ICE1$ (At3g26774), $ICE2$ (At1g12860), and $ACTIN7$ (At5g09810). Sequence data used for hierarchical cluster analysis can be found under the following accession numbers: $CRF1$ (At4g11140), $CRF5$ (At2g46310), $CRF6$ (At3g61630), $CRF7$ (At1g22985), $CRF8$ (At1g71130), $CRF10$ (At1g68550), $CRF11$ (At3g25890),

CRF12 (At1g25470), *ARR7* (At1g19050), *ARR22* (At3g04280), *AHK4* (At2g01830), *ARF7* (At5g20730), and *ARF19* (At1g19220).

Supplemental Data

Supplemental Figure 1. Analysis of the Subcellular Distribution of EGFP:CRF2 and EGFP:CRF3 in Wild-Type Arabidopsis Mesophyll Protoplasts.

Supplemental Figure 2. RT-qPCR Analysis of *ARR1* Expression in *arr1-3* Mutants and *Pro$_{35S}$:10xMYC:ARR1(ARR1OX)/arr1-3* Transgenic Arabidopsis in Response to Cold.

Supplemental Figure 3. PCR Analysis of *crf2-2*, *crf3-2*, *crf3-3*, *crf2-2 crf3-2*, *crf2-2 crf3-3* Mutants and *Pro$_{35S}$:3xHA:CRF2* and *Pro$_{35S}$:3xHA:CRF3* Transgenic Arabidopsis.

Supplemental Figure 4. Root Lengths and LR Densities of Wild-Type, *crf3-2*, and *Pro$_{CRF3}$:CRF3:3xHA/crf3-2* Transgenic Arabidopsis.

Supplemental Figure 5. Analysis of LRP Density at Stage I of Wild-Type, *crf3-2* Mutants, and *Pro$_{CRF3}$:CRF3:3xHA/crf3-2* Transgenic Arabidopsis.

Supplemental Figure 6. Analysis of Cold Response of *Pro$_{CRF2}$:EGFP:GUS* and *Pro$_{CRF3}$:EGFP:GUS* Transgenic Arabidopsis.

Supplemental Figure 7. RT-qPCR Analysis of *CRF2* and *CRF3* Expression in *ice1-2* and *ice2* Mutant Backgrounds Compared with the Wild Type in Response to Cold.

Supplemental Figure 8. Hierarchical Cluster Analysis of *CRF* Genes in a Variety of Arabidopsis Mutants in Response to Phytohormones.

Supplemental Figure 9. ANOVA Tables for Analyses Reported in Figures 1C, 2, 3A, 3C, 5B, 5C, 6B, 7C, and 7D and Supplemental Figures 4B, 4C, and 5.

Supplemental Table 1. Oligonucleotides and PCR Conditions.

Supplemental Table 2. Sequences for the DNA Probes Used in EMSA

AUTHOR CONTRIBUTIONS

J.J., C.C., M.R.L., and N.V.B. designed and conducted the experiments and analyzed the data. J.J. wrote the article. J.K. conceived the project, designed the experiments, analyzed the data, and wrote and edited the article.

REFERENCES

Berckmans, B., et al. (2011). Auxin-dependent cell cycle reactivation through transcriptional regulation of *Arabidopsis* E2Fa by lateral organ boundary proteins. Plant Cell **23:** 3671–3683.

Bielach, A., Podlesáková, K., Marhavy, P., Duclercq, J., Cuesta, C., Müller, B., Grunewald, W., Tarkowski, P., and Benková, E. (2012). Spatiotemporal regulation of lateral root organogenesis in *Arabidopsis* by cytokinin. Plant Cell **24:** 3967–3981.

Blake, W.J., Kærn, M., Cantor, C.R., and Collins, J.J. (2003). Noise in eukaryotic gene expression. Nature **422:** 633–637.

Chang, L., Ramireddy, E., and Schmülling, T. (2015). Cytokinin as a positional cue regulating lateral root spacing in *Arabidopsis.* J. Exp. Bot. **66:** 4759–4768.

Dastidar, M.G., Jouannet, V., and Maizel, A. (2012). Root branching: mechanisms, robustness, and plasticity. Wiley Interdiscip. Rev. Dev. Biol. **1:** 329–343.

De Rybel, B., et al. (2010). A novel aux/IAA28 signaling cascade activates GATA23-dependent specification of lateral root founder cell identity. Curr. Biol. **20:** 1697–1706.

De Smet, I., et al. (2010). Bimodular auxin response controls organogenesis in *Arabidopsis.* Proc. Natl. Acad. Sci. USA **107:** 2705–2710.

Franco-Zorrilla, J.M., López-Vidriero, I., Carrasco, J.L., Godoy, M., Vera, P., and Solano, R. (2014). DNA-binding specificities of plant transcription factors and their potential to define target genes. Proc. Natl. Acad. Sci. USA **111:** 2367–2372.

Fukaki, H., Tameda, S., Masuda, H., and Tasaka, M. (2002). Lateral root formation is blocked by a gain-of-function mutation in the SOLITARY-ROOT/IAA14 gene of *Arabidopsis.* Plant J. **29:** 153–168.

Fursova, O.V., Pogorelko, G.V., and Tarasov, V.A. (2009). Identification of ICE2, a gene involved in cold acclimation which determines freezing tolerance in *Arabidopsis thaliana.* Gene **429:** 98–103.

Goh, T., Kasahara, H., Mimura, T., Kamiya, Y., and Fukaki, H. (2012). Multiple AUX/IAA-ARF modules regulate lateral root formation: the role of *Arabidopsis* SHY2/IAA3-mediated auxin signalling. Philos. Trans. R. Soc. Lond. B Biol. Sci. **367:** 1461–1468.

Hochholdinger, F., and Zimmermann, R. (2008). Conserved and diverse mechanisms in root development. Curr. Opin. Plant Biol. **11:** 70–74.

Horák, J., Grefen, C., Berendzen, K.W., Hahn, A., Stierhof, Y.D., Stadelhofer, B., Stahl, M., Koncz, C., and Harter, K. (2008). The *Arabidopsis thaliana* response regulator ARR22 is a putative AHP phospho-histidine phosphatase expressed in the chalaza of developing seeds. BMC Plant Biol. **8:** 77.

Hosoda, K., Imamura, A., Katoh, E., Hatta, T., Tachiki, M., Yamada, H., Mizuno, T., and Yamazaki, T. (2002). Molecular structure of the GARP family of plant Myb-related DNA binding motifs of the Arabidopsis response regulators. Plant Cell **14:** 2015–2029.

Hwang, I., Sheen, J., and Müller, B. (2012). Cytokinin signaling networks. Annu. Rev. Plant Biol. **63:** 353–380.

Imamura, A., Kiba, T., Tajima, Y., Yamashino, T., and Mizuno, T. (2003). *In vivo* and *in vitro* characterization of the ARR11 response regulator implicated in the His-to-Asp phosphorelay signal transduction in *Arabidopsis thaliana.* Plant Cell Physiol. **44:** 122–131.

Inoue, T., Higuchi, M., Hashimoto, Y., Seki, M., Kobayashi, M., Kato, T., Tabata, S., Shinozaki, K., and Kakimoto, T. (2001). Identification of CRE1 as a cytokinin receptor from *Arabidopsis.* Nature **409:** 1060–1063.

Jefferson, R., and Wilson, K. (1991). The GUS gene fusion system. Plant Mol. Biol. Manual **B14:** 1–33.

Jeon, J., and Kim, J. (2011). FVE, an *Arabidopsis* homologue of the retinoblastoma-associated protein that regulates flowering time and cold response, binds to chromatin as a large multiprotein complex. Mol. Cells **32:** 227–234.

Jeon, J., and Kim, J. (2013). Arabidopsis response Regulator1 and Arabidopsis histidine phosphotransfer Protein2 (AHP2), AHP3, and AHP5 function in cold signaling. Plant Physiol. **161:** 408–424.

Jeon, J., Kim, N.Y., Kim, S., Kang, N.Y., Novák, O., Ku, S.J., Cho, C., Lee, D.J., Lee, E.J., Strnad, M., and Kim, J. (2010). A subset of cytokinin two-component signaling system plays a role in cold temperature stress response in *Arabidopsis.* J. Biol. Chem. **285:** 23371–23386.

Kakimoto, T. (2003). Perception and signal transduction of cytokinins. Annu. Rev. Plant Biol. **54:** 605–627.

Kang, N.Y., Cho, C., Kim, N.Y., and Kim, J. (2012). Cytokinin receptor-dependent and receptor-independent pathways in the dehydration response of *Arabidopsis thaliana.* J. Plant Physiol. **169:** 1382–1391.

Kang, N.Y., Lee, H.W., and Kim, J. (2013). The AP2/EREBP gene PUCHI co-acts with LBD16/ASL18 and LBD18/ASL20 downstream of ARF7 and ARF19 to regulate lateral root development in *Arabidopsis.* Plant Cell Physiol. **54:** 1326–1334.

Kiba, T., Aoki, K., Sakakibara, H., and Mizuno, T. (2004). Arabidopsis response regulator, ARR22, ectopic expression of which results in phenotypes similar to the *wol* cytokinin-receptor mutant. Plant Cell Physiol. **45:** 1063–1077.

Kiba, T., Yamada, H., Sato, S., Kato, T., Tabata, S., Yamashino, T., and Mizuno, T. (2003). The type-A response regulator, ARR15, acts as a negative regulator in the cytokinin-mediated signal transduction in *Arabidopsis thaliana.* Plant Cell Physiol. **44:** 868–874.

Laplaze, L., et al. (2007). Cytokinins act directly on lateral root founder cells to inhibit root initiation. Plant Cell **19:** 3889–3900.

Lavenus, J., Goh, T., Roberts, I., Guyomarc'h, S., Lucas, M., De Smet, I., Fukaki, H., Beeckman, T., Bennett, M., and Laplaze, L. (2013). Lateral root development in *Arabidopsis*: fifty shades of auxin. Trends Plant Sci. **18:** 450–458.

Lee, B.H., Henderson, D.A., and Zhu, J.K. (2005). The *Arabidopsis* cold-responsive transcriptome and its regulation by ICE1. Plant Cell **17:** 3155–3175.

Lee, D.J., Kim, S., Ha, Y.M., and Kim, J. (2008). Phosphorylation of Arabidopsis response regulator 7 (ARR7) at the putative phospho-accepting site is required for ARR7 to act as a negative regulator of cytokinin signaling. Planta **227:** 577–587.

Lee, D.J., Park, J.W., Lee, H.W., and Kim, J. (2009a). Genome-wide analysis of the auxin-responsive transcriptome downstream of iaa1 and its expression analysis reveal the diversity and complexity of auxin-regulated gene expression. J. Exp. Bot. **60:** 3935–3957.

Lee, D.J., Park, J.Y., Ku, S.J., Ha, Y.M., Kim, S., Kim, M.D., Oh, M.H., and Kim, J. (2007). Genome-wide expression profiling of ARABIDOPSIS RESPONSE REGULATOR 7(ARR7) overexpression in cytokinin response. Mol. Genet. Genomics **277:** 115–137.

Lee, H.W., Cho, C., and Kim, J. (2015). *Lateral Organ Boundaries Domain16 and 18* act downstream of the AUX1 and LAX3 auxin influx carriers to control lateral root development in *Arabidopsis thaliana.* Plant Physiol. **168:** 1792–1806.

Lee, H.W., and Kim, J. (2013). *EXPANSINA17* up-regulated by LBD18/ASL20 promotes lateral root formation during the auxin response. Plant Cell Physiol. **54:** 1600–1611.

Lee, H.W., Kim, M.J., Kim, N.Y., Lee, S.H., and Kim, J. (2013). LBD18 acts as a transcriptional activator that directly binds to the *EXPANSIN14* promoter in promoting lateral root emergence of *Arabidopsis.* Plant J. **73:** 212–224.

Lee, H.W., Kim, N.Y., Lee, D.J., and Kim, J. (2009b). *LBD18/ASL20* regulates lateral root formation in combination with *LBD16/ASL18* downstream of *ARF7* and *ARF19* in *Arabidopsis.* Plant Physiol. **151:** 1377–1389.

Licausi, F., Ohme-Takagi, M., and Perata, P. (2013). APETALA2/ Ethylene Responsive Factor (AP2/ERF) transcription factors: mediators of stress responses and developmental programs. New Phytol. **199:** 639–649.

Malamy, J.E., and Benfey, P.N. (1997). Organization and cell differentiation in lateral roots of *Arabidopsis thaliana.* Development **124:** 33–44.

Mizoi, J., Shinozaki, K., and Yamaguchi-Shinozaki, K. (2012). AP2/ERF family transcription factors in plant abiotic stress responses. Biochim. Biophys. Acta **1819:** 86–96.

Nagel, K.A., et al. (2009). Temperature responses of roots: impact on growth, root system architecture and implications for phenotyping. Funct. Plant Biol. **36:** 947–959.

Okushima, Y., Fukaki, H., Onoda, M., Theologis, A., and Tasaka, M. (2007). ARF7 and ARF19 regulate lateral root formation via direct activation of *LBD/ASL* genes in *Arabidopsis.* Plant Cell **19:** 118–130.

Pahlavanian, A.M., and Silk, W.K. (1988). Effect of temperature on spatial and temporal aspects of growth in the primary maize root. Plant Physiol. **87:** 529–532.

Parizot, B., et al. (2008). Diarch symmetry of the vascular bundle in Arabidopsis root encompasses the pericycle and is reflected in distich lateral root initiation. Plant Physiol. **146:** 140–148.

Park, J.Y., Kim, H.J., and Kim, J. (2002). Mutation in domain II of IAA1 confers diverse auxin-related phenotypes and represses auxin-activated expression of *Aux/IAA* genes in steroid regulator-inducible system. Plant J. **32:** 669–683.

Péret, B., De Rybel, B., Casimiro, I., Benková, E., Swarup, R., Laplaze, L., Beeckman, T., and Bennett, M.J. (2009a). *Arabidopsis* lateral root development: an emerging story. Trends Plant Sci. **14:** 399–408.

Péret, B., Larrieu, A., and Bennett, M.J. (2009b). Lateral root emergence: a difficult birth. J. Exp. Bot. **60:** 3637–3643.

Péret, B., et al. (2012). Auxin regulates aquaporin function to facilitate lateral root emergence. Nat. Cell Biol. **14:** 991–998.

Pils, B., and Heyl, A. (2009). Unraveling the evolution of cytokinin signaling. Plant Physiol. **151:** 782–791.

Raines, T., Shanks, C., Cheng, C.Y., McPherson, D., Argueso, C.T., Kim, H.J., Franco-Zorrilla, J.M., López-Vidriero, I., Solano, R., Vaňková, R., Schaller, G.E., and Kieber, J.J. (2016). The cytokinin response factors modulate root and shoot growth and promote leaf senescence in Arabidopsis. Plant J. **85:** 134–147.

Raj, A., Rifkin, S.A., Andersen, E., and van Oudenaarden, A. (2010). Variability in gene expression underlies incomplete penetrance. Nature **463:** 913–918.

Rashotte, A.M., and Goertzen, L.R. (2010). The CRF domain defines cytokinin response factor proteins in plants. BMC Plant Biol. **10:** 74.

Rashotte, A.M., Mason, M.G., Hutchison, C.E., Ferreira, F.J., Schaller, G.E., and Kieber, J.J. (2006). A subset of *Arabidopsis* AP2 transcription factors mediates cytokinin responses in concert with a two-component pathway. Proc. Natl. Acad. Sci. USA **103:** 11081–11085.

Riefler, M., Novak, O., Strnad, M., and Schmülling, T. (2006). *Arabidopsis* cytokinin receptor mutants reveal functions in shoot growth, leaf senescence, seed size, germination, root development, and cytokinin metabolism. Plant Cell **18:** 40–54.

Sakai, H., Aoyama, T., and Oka, A. (2000). *Arabidopsis* ARR1 and ARR2 response regulators operate as transcriptional activators. Plant J. **24:** 703–711.

Shi, Y., Tian, S., Hou, L., Huang, X., Zhang, X., Guo, H., and Yang, S. (2012). Ethylene signaling negatively regulates freezing tolerance by repressing expression of CBF and type-A ARR genes in *Arabidopsis.* Plant Cell **24:** 2578–2595.

Shibasaki, K., Uemura, M., Tsurumi, S., and Rahman, A. (2009). Auxin response in *Arabidopsis* under cold stress: underlying molecular mechanisms. Plant Cell **21:** 3823–3838.

Šimášková, M., et al. (2015). Cytokinin response factors regulate *PIN-FORMED* auxin transporters. Nat. Commun. **6:** 8717.

Suzuki, T., Miwa, K., Ishikawa, K., Yamada, H., Aiba, H., and Mizuno, T. (2001). The *Arabidopsis* sensor His-kinase, AHk4, can respond to cytokinins. Plant Cell Physiol. **42:** 107–113.

Swarup, K., et al. (2008). The auxin influx carrier LAX3 promotes lateral root emergence. Nat. Cell Biol. **10:** 946–954.

Tian, H., De Smet, I., and Ding, Z. (2014). Shaping a root system: regulating lateral versus primary root growth. Trends Plant Sci. **19:** 426–431.

Tiwari, S.B., Hagen, G., and Guilfoyle, T. (2003). The roles of auxin response factor domains in auxin-responsive transcription. Plant Cell **15:** 533–543.

To, J.P., Haberer, G., Ferreira, F.J., Deruère, J., Mason, M.G., Schaller, G.E., Alonso, J.M., Ecker, J.R., and Kieber, J.J. (2004). Type-A Arabidopsis response regulators are partially redundant negative regulators of cytokinin signaling. Plant Cell **16:** 658–671.

To, J.P., and Kieber, J.J. (2008). Cytokinin signaling: two-components and more. Trends Plant Sci. **13:** 85–92.

Ueguchi, C., Sato, S., Kato, T., and Tabata, S. (2001). The AHK4 gene involved in the cytokinin-signaling pathway as a direct receptor molecule in *Arabidopsis thaliana.* Plant Cell Physiol. **42:** 751–755.

Ulmasov, T., Hagen, G., and Guilfoyle, T.J. (1997). ARF1, a transcription factor that binds to auxin response elements. Science **276:** 1865–1868.

Vanneste, S., et al. (2005). Cell cycle progression in the pericycle is not sufficient for SOLITARY ROOT/IAA14-mediated lateral root initiation in *Arabidopsis thaliana.* Plant Cell **17:** 3035–3050.

Yamada, H., Suzuki, T., Terada, K., Takei, K., Ishikawa, K., Miwa, K., Yamashino, T., and Mizuno, T. (2001). The *Arabidopsis* AHK4 histidine kinase is a cytokinin-binding receptor that transduces cytokinin signals across the membrane. Plant Cell Physiol. **42:** 1017–1023.

Zhu, J., Zhang, K.X., Wang, W.S., Gong, W., Liu, W.C., Chen, H.G., Xu, H.H., and Lu, Y.T. (2015). Low temperature inhibits root growth by reducing auxin accumulation via *ARR1/12.* Plant Cell Physiol. **56:** 727–736.

Zwack, P.J., Compton, M.A., Adams, C.I., and Rashotte, A.M. (2016). Cytokinin response factor 4 (CRF4) is induced by cold and involved in freezing tolerance. Plant Cell Rep. **35:** 573–584.

Zwack, P.J., Shi, X., Robinson, B.R., Gupta, S., Compton, M.A., Gerken, D.M., Goertzen, L.R., and Rashotte, A.M. (2012). Vascular expression and C-terminal sequence divergence of cytokinin response factors in flowering plants. Plant Cell Physiol. **53:** 1683–1695.